

DOI: 10.1002/adfm.200700972

Nanocomposite Films of a Polyfluorene Copolymer and Carbazole–Thiol-Capped Gold Nanoparticles: Electrochemical Crosslinking and Energy-Transfer Properties**

By Prasad Taranekar, Chengyu Huang, Timothy M. Fulghum, Akira Baba, Guoqian Jiang, Jin-Young Park, and Rigoberto C. Advincula

The preparation and properties of an electrochemically crosslinked Au nanoparticle/polyvinylcarbazole (PVK)/polyfluorene (PFC) nanocomposite film is described. Blends of the blue-light emitting PFC, PVK, and the 11-(9H-carbazol-9-yl)-undecane-1-thiol-capped Au nanoparticles (CBZ-S-Au) were prepared as thin films by spin-coating and subsequent crosslinking by cyclic voltammetry (CV). The electrochemical properties are then evaluated on the basis of the redox behavior (reversibility) and electron-transport properties of the films. They are further characterized by UV-vis spectroscopy, photoluminescence spectroscopy, and atomic force microscopy (AFM). The large differences in photoluminescence properties of the CBZ-S-Au/PFCVK crosslinked copolymer composite film compared to the PFCVK polymer alone result in an efficient energy-transfer system, in which the excimer peak is almost totally quenched. This indicates a compatible match between the absorbance of the Au plasmons and the emission of the excimer energy trap from PF polymers. Furthermore, electrochemical crosslinking enhances this match both by shifting the absorbance to greater overlap and decreasing the Förster distance between the Au nanoparticle and the PFCVK polymer chains.

1. Introduction

Composites and nanocomposites have been the focus of much research for developing new and smart polymer materials.^[1] A major objective is to obtain a property (or a combination of properties) not available in any of the individual components. Improved mechanical properties or processability is desirable. Recently, polymer composites with high electrical and thermal conductivities have also been targeted towards novel electro-optical applications.^[2,3] Nanocomposites consisting of inorganic nanoparticles and organic polymers often exhibit a host of mechanical, electrical, optical, and magnetic properties that are far superior when compared with their original polymer hosts.^[4] It has been reported earlier that the luminescence properties of a light-emitting polymer doped with metal nanoshells or metal nanoparticles were enhanced

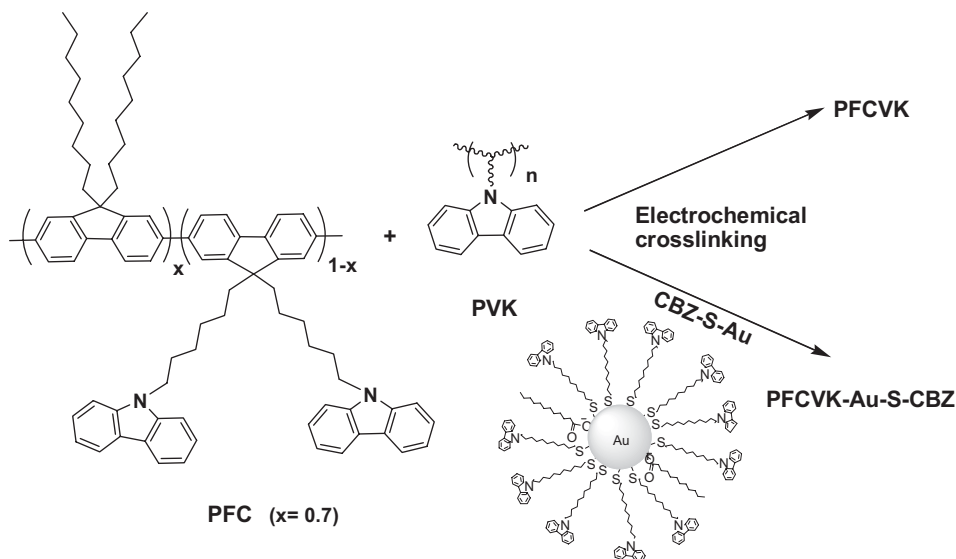
because of the quenching of triplet excitons, whose energy levels overlap with the absorption bands of the metal nanoshells or metal nanoparticles.^[5,6]

Au nanoparticles to date have been one of the most well-studied materials, not only because of the ease of their synthesis but also because of their surface plasmon properties and amenability to surface functionalization.^[7] Their contributions towards fluorescence quenching and enhancement of Raman spectroscopic intensities are also well-known.^[8] These nanoparticles are often coated with dispersing agents, such as alkane-thiols or polyvinylpyrrolidone in order to distribute them well in a polymer matrix. Because of this additional nonconjugated dispersing agent and phase-segregation tendencies, the electrical resistance and threshold voltage of devices fabricated with such polymer/nanoparticle composite materials are increased.^[9] Therefore, to improve these properties, our group has attempted to circumvent this problem by incorporating ligand-exchanged carbazole-functionalized Au nanoparticles (NPs) via electrochemical crosslinking of the carbazole moieties with PVK [poly(9-vinylcarbazole)] and polyfluorene (PFC) copolymer derivatives (Scheme 1). The interest mainly lies in two objectives: 1) electropolymerizability of a ternary composition for uniform blending and 2) energy-transfer properties of an electrochemically crosslinked conjugated polymer network nanocomposite.

PVK is a hole-transporting organic semiconducting polymer.^[10] It has a wide bandgap energy (E_g) and has been widely used as an electronic and optical material. It can be blended with light-emitting polymers to introduce higher luminescence efficiency than the homopolymer alone.^[11,12] On the other

[*] Dr. R. C. Advincula, Dr. P. Taranekar, C. Huang, Dr. T. M. Fulghum, Dr. A. Baba, G. Jiang, and J. Y. Park
Department of Chemistry, 136 Fleming Building
University of Houston
Houston, TX 77204-5003 (USA)
E-mail: radvincula@uh.edu

[**] The authors gratefully acknowledge partial funding from the Robert E. Welch Foundation (E-1551), the National Science Foundation (NSF DMR-0602896 and NSF-CTS 0330127), and technical support from Optrel GmbH, Agilent Technologies, and Varian Inc.



Scheme 1. Preparation of crosslinked polycarbazole films with (forming PFCVK–Au–S–CBZ) and without gold nanoparticles (forming PFCVK).

hand, p-conjugated polyfluorene (PF) has been used extensively to prepare organic light-emitting diodes (LEDs) because of interest in blue-emitting materials.^[13,14] However, these polymers have a higher bandgap than most emissive polymers and are prone to excitonic quenching because of the tendency to aggregate (or crystallize) in films.^[15]

Our group has previously designed a polyfluorene derivative with a pendant carbazole group that can be electrochemically grafted to a carbazole alkylsilane self-assembled monolayer (SAM).^[14] Using this method, the results showed a decrease in the excimer peak because of aggregation leading to higher luminescence efficiencies. It is anticipated that if this polymer can be co-electropolymerized in a physical blend with PVK, improved thermal stability, excellent film-forming properties, and a high emission quantum yield can be expected. It is also believed that such blending will not only lead to new methods for fabricating flexible polymer LEDs (PLEDs) but also result in improved devices with increased oxidative stability and work function tunability.^[16]

This approach is analogous to what has been previously reported by our group and others as a “precursor polymer” approach for forming conjugated-polymer networks (CPNs).^[16] The main difference is the incorporation of functionalized Au nanoparticles with electrochemically active ligand groups and their electro-optical effects. Although in the past blends of fluorene polymers and gold nanoparticles have been reported,^[17] the long-lived excitons of polyfluorene were not effectively quenched. In the present study, the efficient quenching by the donor–acceptor interaction of gold nanoparticles and polyfluorene with pendant carbazole/PVK (PFCVK) cross-linked nanocomposite films is demonstrated. This leads to purer blue emission by reducing the yellow/green excimer hue of the photoluminescence. It is believed that an electrochemical crosslinking approach coupled with Au nanoparticles will

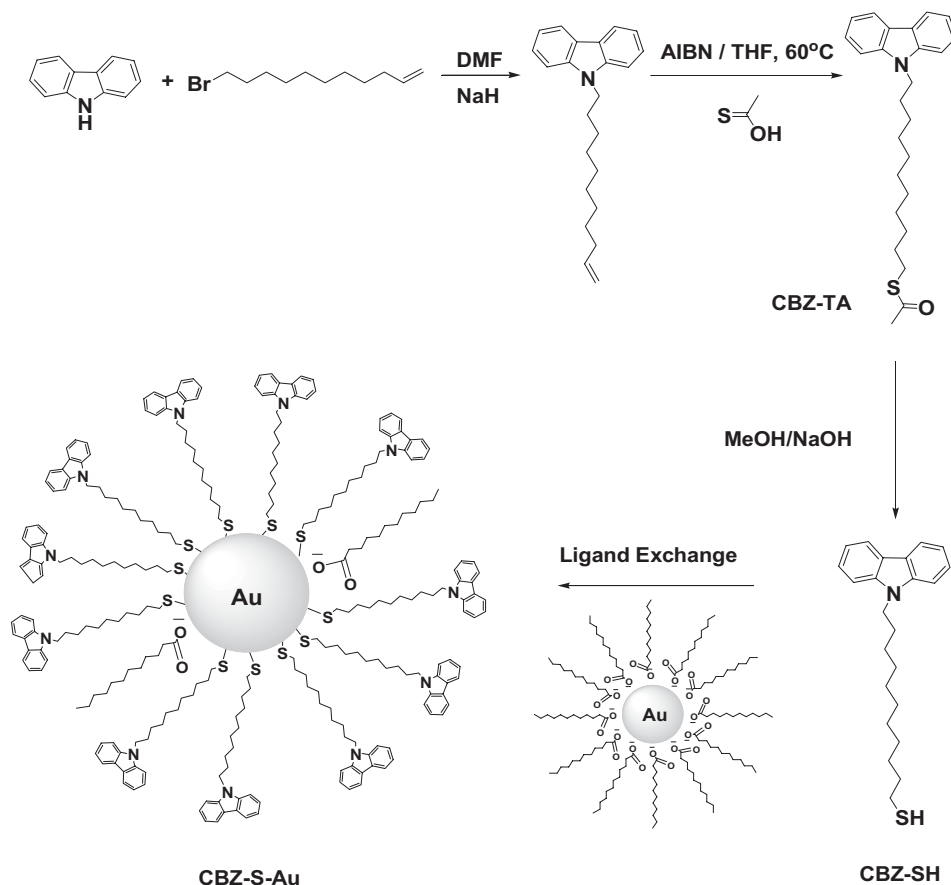
lead to composite films with high thermal stability and should exhibit interesting electro-optical behavior when applied to PLED devices.

2. Results and Discussion

2.1. Absorption Studies and Transmission Electron Microscopy

Composite films based on carbazole–thiol-capped Au nanoparticles (CBZ-S-Au) were made and could be fabricated as ultrathin films on electrode surfaces. The synthesis scheme is shown in Schemes 1 and 2. A strong absorption band at around 530 nm arises from the surface plasmon of the Au nanoparticles, as shown in Figure 1, indicating that the diameter of the particles is greater than 5 nm.^[18–20] Carbazole–thiol ligands were then exchanged onto the gold nanoparticles to form the CBZ-S-Au (Scheme 2). The UV-vis spectrum shows two absorption peaks at 346 and 541 nm. The ligand itself (CBZ-SH) has an absorption band at 346 nm, which is retained after ligand exchange with the Au nanoparticles (CBZ-S-Au) along with the plasmon peak, which is shifted from 531 to 541 nm. This 10 nm red-shift is presumably a result of ligand exchange and repeated precipitation/redispersion cycles, which can cause some aggregation of the nanoparticles.^[21,22]

The transmission electron microscopy (TEM) images show a fairly uniform distribution in the NP size (Fig. 2). After ligand exchange, the gold nanoparticles (CBZ-S-Au) showed a mean diameter of 8.2 nm with a standard deviation of ± 1.2 nm. These dimensions and distribution are consistent with that observed from absorbance measurements. Typical surface plasmon resonance of Au nanoparticles with various diameters gives a corresponding UV absorbance band at different wavelength ranges, similar to that reported earlier by Kondow and co-workers.^[23a]



Scheme 2. Preparation of carbazole–thiol ligand-exchanged gold nanoparticles (CBZ-S-Au). See Experimental for further synthesis details.

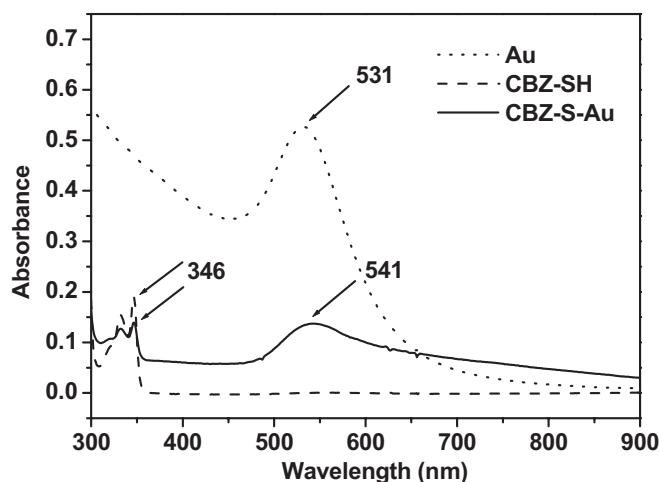
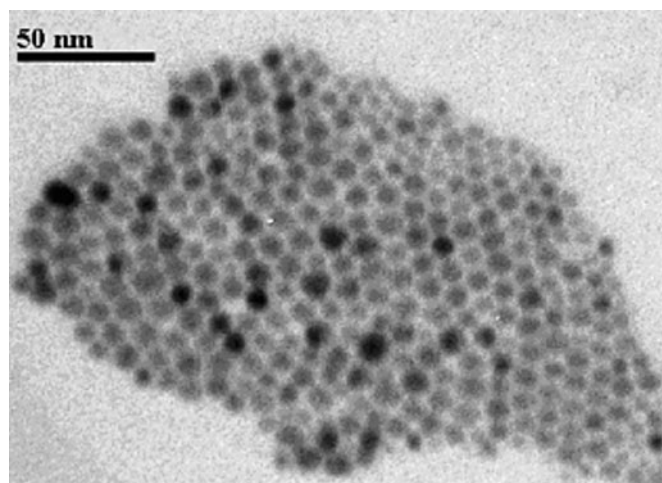


Figure 1. UV-vis absorption spectra of Au nanoparticles, the CBZ-SH ligand, and CBZ-S-Au NPs prepared by ligand exchange.

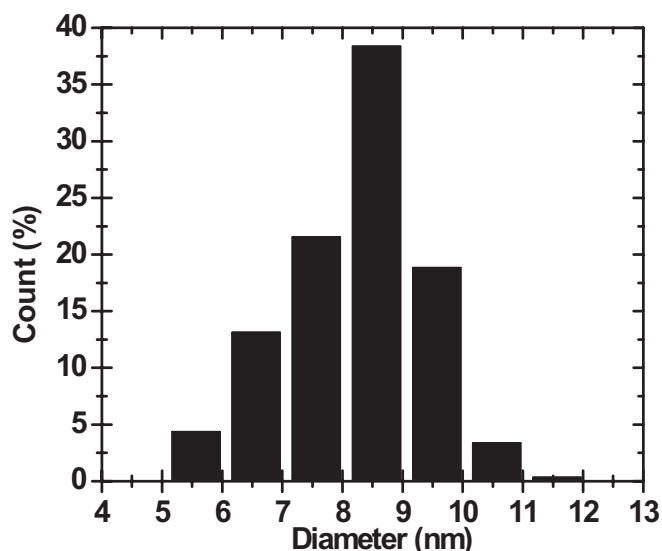
2.2. Electrochemistry

Solutions with composites of PVK and PFC combined with CBZ-S-Au nanoparticles were deposited on indium tin oxide (ITO, Scheme 1). Specifically, the mixtures were spin-coated to form transparent films, which were then electrochemically

crosslinked. Cyclic voltammetry (CV) was performed to cross-link the electroactive carbazole groups in PVK and PFC for five cycles with a scan rate of 20 mV s^{-1} . The anodic peak potential in Figure 3 a and b occurs at 0.65 V, which is related to the oxidation of the conjugated polymer, and the corresponding reduction peak was found to be at 0.55 V.^[14a] As reported in this previous work,^[14a] the peak at 0.78 V (vs. Ag/Ag^+ (0.01 m), not highly resolved) in the first cycle is attributed to the oxidation of the carbazole monomer, while from the second cycle, the peak at around 0.6 V emerges because of the formation of more conjugated species. It is hard to distinguish any major changes in the cyclic voltammograms of the films with and without CBZ-S-Au, as well as by altering the CBZ-S-Au ratios. However, the differences in peak anodic current over the same observed crosslinking area (higher in the case of carbazole-terminated gold NPs) suggests the incorporation of more carbazole groups in the composite material.^[14a] This is reasonable because CBZ-S-Au NPs bearing terminated carbazoles are now participating in the crosslinking event compared to the PFCVK polymer alone. This effect is more distinguished with the higher peak anodic currents observed for the CBZ-S-Au nanocomposite films (Fig. 3b) as opposed to the cyclic voltammogram bearing no carbazole-terminated Au nanoparticles. The gold nanoparticle concentration was optimized to get optically clear films, while at the same time retaining



(a)

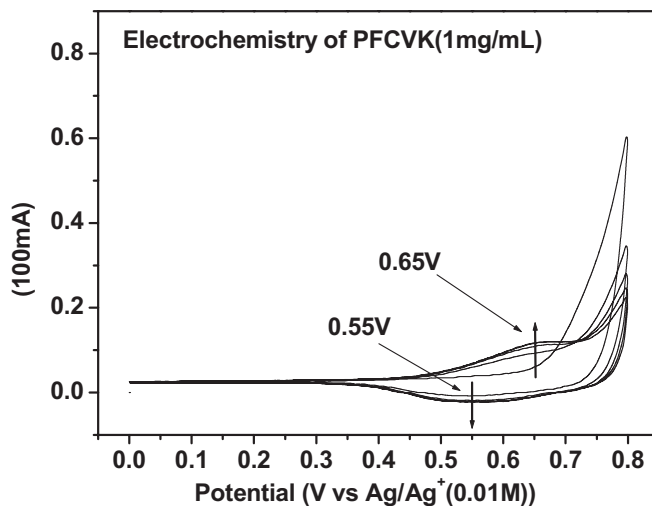


(b)

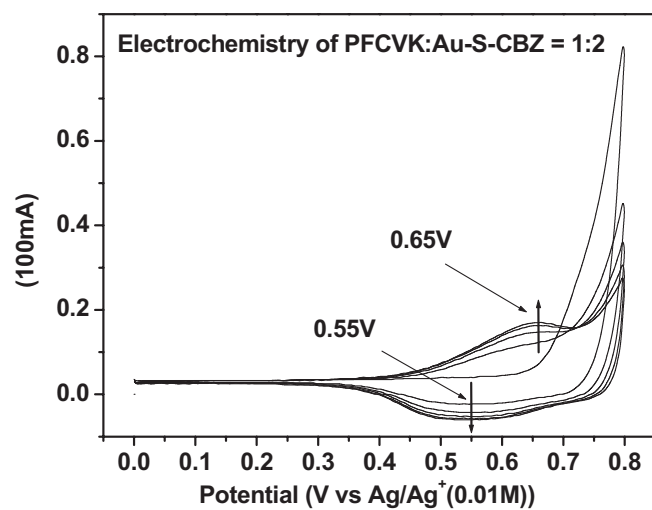
Figure 2. a) Transmission electron image of CBZ-S-Au and b) the corresponding size distribution histogram. The average diameter is 8.2 nm with a standard deviation $\sigma = 0.7$ nm.

their polymer exciton fluorescence intensity. This kind of optical property is in fact desirable for future PLED applications.

After completely crosslinking the film, the monomer free scan rate (v) dependence on current (I) for the electrodeposited PFCVK films was studied on a ~ 45 – 50 nm thick gold substrate, as shown in Figure 4 a and b. The plot of I vs. $v^{1/2}$ (inset) shows a nonlinear relationship, which indicates non-diffusion-controlled kinetic behavior for ion-transport within the films. It is possible that the ion-transport behavior is going towards a surface-limited regime. This can be caused by a gradient in the electro-crosslinking, which tends to be more crosslinked in the first few cycles or near the substrate. On the other hand, PVK and PFC alone have linear I versus $v^{1/2}$ relationships, which show predominantly diffusion-controlled behavior.^[14] What is



(a)



(b)

Figure 3. Cyclic voltammety studies of a) PFCVK and b) PFCVK–Au-S-CBZ composite films with the same working electrode area. The positions of the oxidation and reduction peaks for both systems are shown.

of high interest then is that these materials are not as highly porous as is the case for the pure, individual polymers (both PVK and PFC).

2.3. Photoluminescence

Figure 5 shows the photoluminescence spectra of the four films excited at 380 nm. The well-resolved peaks near 425 and 450 nm result from the emission properties of the polyfluorene backbone, with the (0–0) transition at 425 nm the dominant one.^[23] In addition to these two peaks, the excimers had the typical yellow/green color at 550 nm (no Au nanoparticles).^[24] This excimer peak is an energy trap that results from aggregation in PF polymer films and is not typically observed in solutions as the degree of intermolecular interactions increases in going from solution to solid state.^[23a] It has also been attributed to the formation of fluorenone species in the backbone.^[23b]

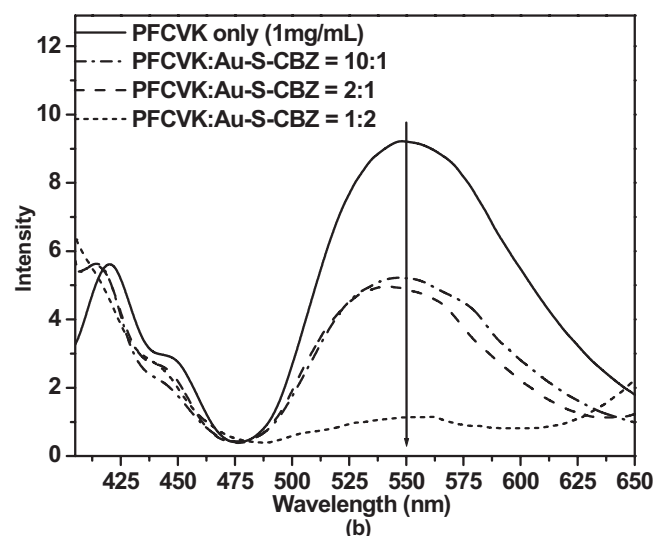
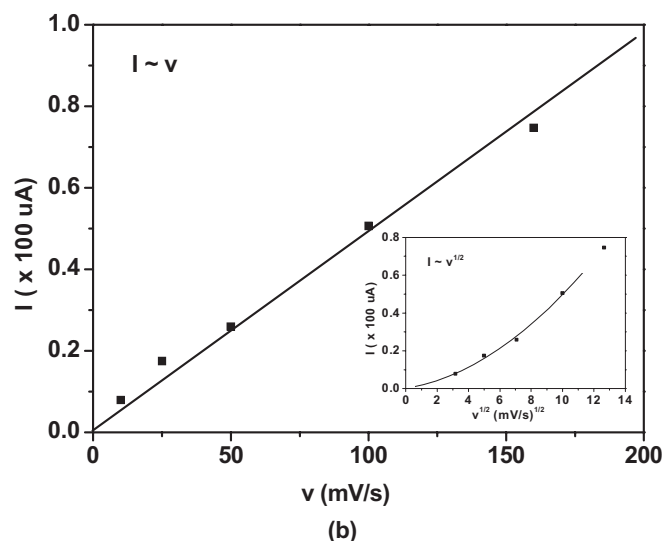
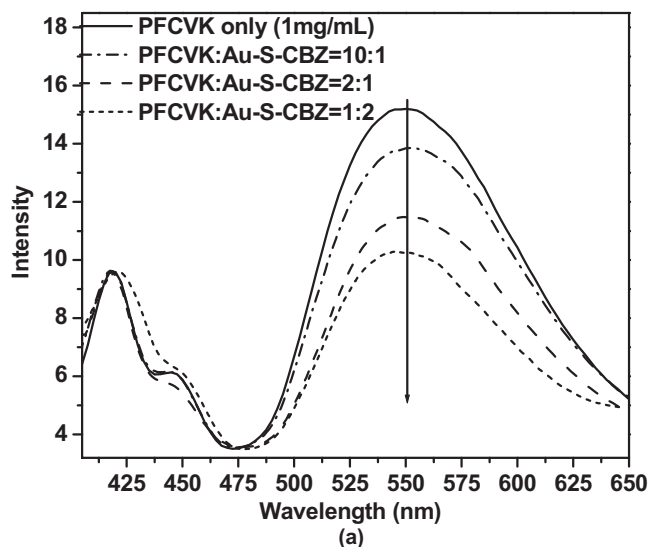
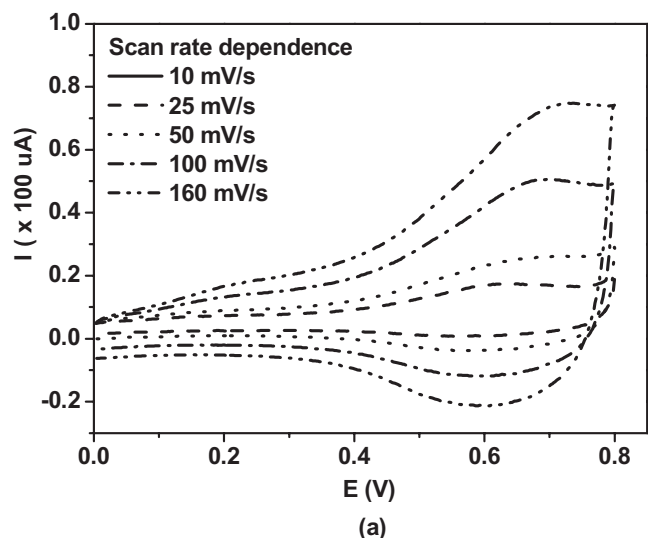


Figure 4. Cyclic voltammetry studies of PFCVK–Au-S-CBZ: a) PFCVK at various scan rates and b) I versus ν plot with inset showing I versus $\nu^{1/2}$.

Figure 5. Photoluminescence spectra of spin-coated PFCVK and PFCVK–Au-S-CBZ composite films a) before and b) after crosslinking.

The introduction of the carbazole group enhanced aggregation of the polymer, leading to a much stronger peak relative to pure PF. By intermixing Au nanoparticles in a blend with PFCVK/CBZ-S-Au with ratios of 10:1, 2:1, and 1:2, an evident decrease of this peak before electrochemistry is observed, as shown in Figure 5a, consistent with the energy transfer of the excitonic peak to the surface plasmon absorption band of the nanoparticles.^[17] This decrease is proportional to the Au nanoparticle content. However, the peak intensity decreases even more significantly upon electrochemical crosslinking. The resulting composite films show that the photoluminescence was quenched by about half in the cases of PFCVK/CBZ-S-Au for both 10:1 and 2:1 ratios after crosslinking. On the other hand, complete quenching was observed when the ratio was as 1:2, as shown in Figure 5b. With this approach, the yellow/green hue of the photoluminescence can be quenched, leading to a purer blue light-emitting material.^[24,25]

The quenching efficiency can be expressed quantitatively by the ratio of green/blue emission after all the blue peaks at 426 nm were normalized. The ratio of green/blue emission is 1.93:1, 1.69:1, 1.31:1, and 1.12:1 before crosslinking, as well as 1.69:1, 0.92:1, 0.88:1, and 0.15:1, respectively, after cyclic voltammetry, for films with increasing Au NP concentrations. The dominant quenching process can have a completely different nature in the presence of gold nanoparticles. Energy transfer requires a good overlap between the absorption of the acceptor and the light-harvesting chromophore (donor). In this case, the Au nanoparticles serve as efficient quenchers of the conjugated-polymer excitonic fluorescence (excimer peak), presumably through long-range resonance energy transfer. Heeger and co-workers demonstrated that long-range energy transfer offers a significant contribution to quenching relative to two other factors: internal energy or electron transfer and the electrostatic interaction between the polymer and the gold nanoparticles.^[26]

In related work done by Gu et al.^[21] where gold nanoparticles were simply mixed with emissive fluorenyl groups, a strong fluorescence emission quenching was observed. However, in the present work the electrochemically crosslinked composite films provide more carbazole groups to connect together and form a continuous phase in a conjugated network, allowing phase mixing and more interaction for a favorable energy transfer.^[16] The crosslinking procedure should also decrease the distance between the Au NP and PFCVK polymer chains. Because the metal nanoparticle resonance has an excitation lifetime of only a few picoseconds,^[17] the donor–acceptor interaction changes brought upon by electrochemical crosslinking quenches the long-lived triplet state of PFCVK more effectively. The distance-dependent quenching should be somewhat similar to that observed in other chromophore-functionalized Au nanoparticles.^[27] Energy transfer between two point dipoles in solutions (Förster type) is known^[28] to vary with the sixth power of the separation distance, whereas energy transfer between a point dipole and a metal surface varies as the third power of the intervening distance. If the energy-transfer distance dependence is as an n^{th} power, then the relation between energy-transfer efficiency and distance can be expressed by:

$$\phi_{\text{ET}} = \frac{1}{1 + (R/R_0)^n} \quad (1)$$

where R is the distance [\AA] between the donor and the acceptor, and R_0 is the critical distance at which ϕ_{ET} is 50 %. From this equation, it is clear that this energy-transfer efficiency increases with decreasing distance, R , between the PFCVK polymer and the Au NP as a result of crosslinking.

Thus, the films that were not subjected to crosslinking, but were physically blended, did not quench as effectively. Moreover, nanocomposites are prone to thermal and long-term instability because of phase separation. It is conceivable that crosslinking not only helps in efficient excimer quenching but also provides robust films.^[16] In principle, further fine tuning is possible with respect to quenching efficiency by a phase-diagram optimization (quenching efficiency versus PFCVK:CBZ-S-Au) of the composition.

2.4. Morphology Studies

It is possible to study the crosslinking of polymers on solid substrates by atomic force microscopy (AFM).^[26] The morphology of spin-coated PFCVK (PFC/PVK = 4:1) films (without gold nanoparticles) before and after electrochemical crosslinking on ITO substrates was examined ($10 \mu\text{m} \times 10 \mu\text{m}$) under magnetic AC (MAC) mode. As seen from Figure 6 a and b, the topographic and phase images before cyclic voltammetry present a roughness of ca. $\sim 6.28 \text{ nm}$. The ellipsoidal domains are most likely attributed to aggregation of PFC–PVK polymers possibly because of nonoptimized spin-coating conditions for this blend composition and the inherent aggregation tendencies of polyfluorene. On the other hand, the complete coverage of the underlying ITO substrate with the polymer

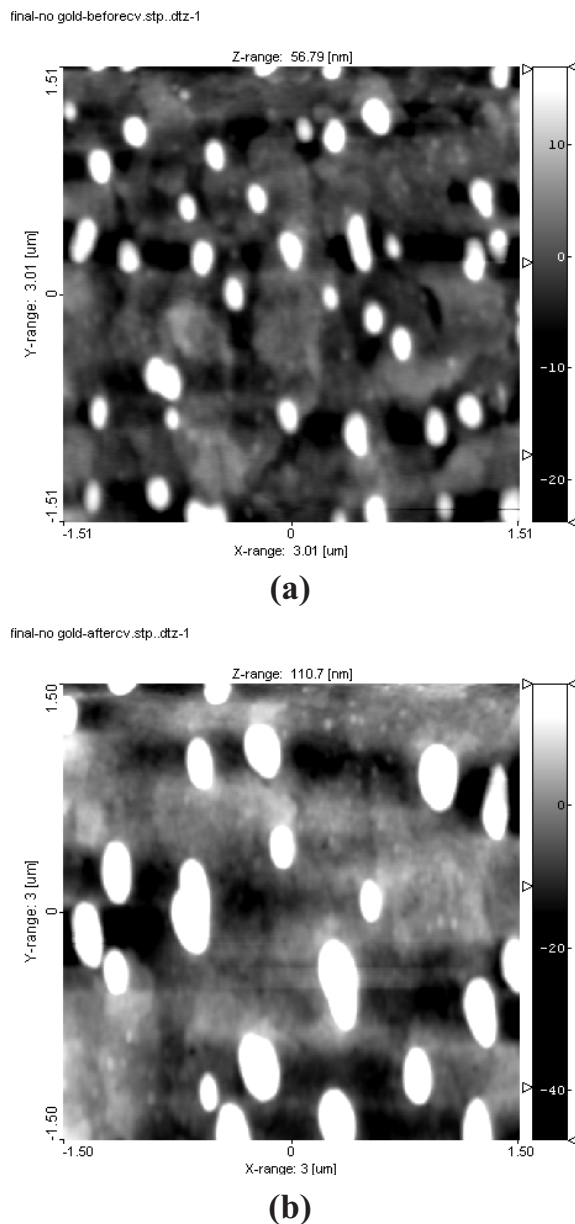


Figure 6. AFM images for PFCVK films. Topographical features of the film a) before and b) after crosslinking.

suggests a good conducting contact for the electrochemical measurements. Note that the surface of the ITO is very different (not shown) and has a roughness of the order of ca. $\sim 9.0 \text{ nm}$. The total film thickness of the spin-coated film is about $\sim 134 \text{ nm}$, by AFM profilometry. After the CV measurements, it is clear that the underlying film became smoother and the domains became larger (compare Fig. 5a and b). The aggregates of PFCVK after CV grew simultaneously with the formation of a more homogeneous and smooth surface on the whole substrate, consistent with the crosslinking process. This morphology should be related to the electrochemical behavior observed by CV. Further optimization of morphology control by using different blend compositions and substrate-wetting

conditions are also underway for the PFCVK–nanoparticle composites.

3. Conclusions

A nanocomposite film was investigated by using a blue-emitting PFCVK copolymer and 11-(9H-carbazol-9-yl) undecane-1-thiol-capped Au nanoparticles. These materials were successfully synthesized, blended, and crosslinked. Ultrathin films of PFCVK with and without CBZ-S-Au were spin-coated and then electrochemically crosslinked. The films were characterized using CV, UV-vis and photoluminescence spectroscopies, and AFM. Electrochemical crosslinking was achieved by CV methods and formed thin nanocomposite films. The large differences in photoluminescence properties of the CBZ-S-Au nanoparticle/PFCVK crosslinked copolymer composite films compared to the PFCVK polymer alone was the result of an efficient energy-transfer system, in which the excimer peak was almost totally quenched. Quantitatively, the blue/green emission was changed from 1.93:1 to 1.69:1 for the PFCVK film, and from 1.12:1 to 0.15:1 for the film with PFCVK/CBZ-S-Au = 1:2. This indicated a compatible match between the absorbance of the Au plasmons and the emission of the excimer energy trap from PF polymers caused by aggregation. Electrochemical crosslinking further enhanced this match by both shifting the absorbance to greater overlap and decreasing the distance between the Au NP and the PFCVK polymer chains. Further work will be done in the future to investigate PLED device characteristics.

4. Experimental

4.1. Chemicals

Poly(9-vinylcarbazole) [number-average molecular weight, M_n = 55 500], tetrabutylammonium borohydride (TBAB, 98 %) and didodecyldimethylammonium bromide (DDAB, 98 %) were purchased from Aldrich. Carbazole (Aldrich, 96 %) and 2,2'-azobisisobutyronitrile (AIBN, Aldrich, 98 %) were recrystallized twice from ethanol. 11-Bromoundec-1-ene (Alfa Aesar, 96 %), AuCl₃ (Alfa Aesar, packed under argon), and thioacetic acid (Acros, 98 %) were used as received. All solvents were dried by conventional procedures and distilled before use. The synthesis of polyfluorene derivatives with carbazole pendant groups (PFC = polyfluorene copolymer) had been previously reported by our group [15c].

4.2. Instrumentation

NMR was carried out by using a General Electric QE 300 spectrometer (¹H 300 MHz). UV-vis spectra were recorded using an Agilent 8453 spectrometer. The average size of the gold nanoparticles was determined using a Hitachi transmission electron microscope (H-7000). Fluorescence spectra were obtained on a Perkin–Elmer LS-45 luminescence spectrometer. Cyclic voltammetry was performed on an Amel 2049 potentiostat and power lab/4SP system with a three-electrode cell. AFM imaging was performed under ambient conditions with a PicoSPM II (PicoPlus, Molecular Imaging) in the magnetic AC mode (MAC mode). MAC mode uses a magnetic field to drive a magnetically

coated cantilever in the top-down configuration. Type II MAC cantilevers with a spring constant of 2.8 nN m⁻¹ and a 10 nm radius tip were used for all scans. The scanning probe imaging processor (SPIP, version 4.0.6.0, Image Metrology Company) was used to analyze the roughness of all AFM images and obtain other information.

4.3. Spin-Coating and Electrochemical Studies

For electrochemical studies, ITO glass substrates were first washed by hand with Alconox detergent, and then rinsed with ultra-pure water (Millipore, 18.2 MΩ cm, with 0.22 μm filter). They were then sonicated in isopropyl alcohol, hexane, and toluene for 10 min in each, followed by treatment with RCA recipe (H₂O/H₂O₂/NH₃ = 10:2:0.6, 55–60 °C, 75 min) and argon/oxygen plasma cleaning. PFC and PVK were then spin-cast onto the ITO substrates from their chloroform solutions with different CBZ-S-Au amounts at 2000 rpm for 2 min to form transparent films. The concentration of PFC and PVK was fixed at 0.067 wt% (1 mg mL⁻¹, PFC/PVK = 4:1) and weight ratios of PFC-PVK/CBZ-S-Au were 10:1, 2:1, and 1:2. After the substrate was dried under nitrogen, it was used as the working electrode for the electrochemical experiment. CV was performed in a three-electrode cell containing 0.1 M tetrabutylammonium hexafluorophosphate (TBAH) acetonitrile solution with platinum as the counter electrode and a Ag/Ag⁺ (0.1 M TBAH and 0.01 M AgNO₃ in acetonitrile) reference electrode, with a potential range from 0 to 800 mV versus the Ag/Ag⁺ reference electrode. After several cycles, the polymer-coated substrate was taken out and rinsed vigorously with methylene chloride, chloroform, and finally with ethanol to remove all the soluble impurities. The substrate was then dried under nitrogen before further characterization.

4.4. Synthesis

4.4.1. Synthesis of 9-(Undec-10-enyl)-9H-carbazole

To a stirred solution of carbazole (6.00 g, 35.9 mmol) in dimethylformamide (DMF, 15 mL), NaH (0.950 g, 39.6 mmol) was added in portions and after complete addition, the mixture was heated to 60 °C for 2 h. After the mixture was cooled, a solution of 11-bromoundec-1-ene (9.40 g, 40.5 mmol) in DMF (5 mL) was added dropwise to the reaction mixture and was stirred for 48 h at room temperature. The reaction mixture was then poured in water and was extracted using methylene chloride and dried over Na₂SO₄. After evaporating the solvent, the crude product was purified by column chromatography using hexane as an eluent. This yielded 9.50 g (82.6 %) of the product. ¹H NMR (CDCl₃) δ: 8.14 (d, 2H), 7.53–7.42 (m, 4H), 7.27 (t, 2H), 5.80 (m, 1H), 4.95 (t, 2H), 4.29 (t, 2H), 2.02 (p, 2H), 1.86 (p, 2H), 1.35–1.22 ppm (m, 12H). ¹³C NMR δ: 140.6, 139.3, 125.7, 123.1, 120.3, 118.9, 114.3, 109.9, 43.4, 34.2, 29.8, 29.7, 29.4, 29.3, 29.2, 27.7 ppm.

4.4.2. Synthesis of 11-(9H-Carbazol-9-yl)undecyl ethanethioate (CBZ-TA)

The synthesis of CBZ-TA was accomplished by a modified procedure from Luk et al. [29]. A solution of 9-(undec-10-enyl)-9H-carbazole (1.91 g, 5.98 mmol) in dry tetrahydrofuran (THF, 20 mL) containing thioacetic acid (0.630 g, 8.29 mmol) and AIBN (56.0 mg, 0.341 mmol) was refluxed at 60 °C for 12 h. After cooling the reaction flask, AIBN (20 mg) and thioacetic acid (30 mg) were added and refluxed for another 4 h. Rotary evaporation of the solvent from the reaction mixture followed by flash column chromatography (hexane/CH₂Cl₂, 4:1) gave 2.10 g (88.6 %) of the product. ¹H NMR (CDCl₃) δ: 8.14 (d, 2H), 7.53–7.42 (m, 4H), 7.27 (t, 2H), 4.29 (t, 2H), 2.70 (t, 2H), 2.35 (s, 3H), 1.92–1.88 (m, 2H), 1.74–1.69 (m, 2H), 1.38–1.26 ppm (m, 14H). ¹³C NMR δ: 196, 140.6, 125.7, 123.1, 120.3, 118.6, 108.9, 43.0, 39.1, 35.1, 32.1, 30.5, 29.4, 29.3, 29.1, 28.9, 27.3 ppm.

4.4.3. Synthesis of 11-(9H-Carbazol-9-yl)undecane-1-thiol (CBZ-SH)

CBZ-TA (1.00 g, 2.53 mmol) was dissolved in methanol (10 mL) in a 100 mL round-bottom flask. Methylene chloride was added dropwise to make the suspension clear. To this solution, sodium hydroxide solution (1 mL, 50 wt%) was added under nitrogen and stirred overnight. The reaction mixture was neutralized by adding acetic acid. The neutralized solution was then poured into 25 mL of water and the organic phase was extracted using methylene chloride. The organic phase was then washed with brine and dried over Na₂SO₄. After filtering and concentrating under vacuum, the crude product was further washed with hexane to give the pure product as 780 mg (87.6 %) of slightly yellowish oil. ¹H NMR (CDCl₃) δ: 8.14 (d, 2H), 7.53–7.42 (m, 4H), 7.27 (t, 2H), 4.29 (t, 2H), 2.68 (t, 2H), 1.92–1.88 (m, 2H), 1.74–1.69 (m, 2H), 1.38–1.26 ppm (m, 15H). ¹³C NMR δ: 140.6, 125.7, 123.1, 120.3, 118.6, 108.9, 43.0, 39.1, 35.1, 32.1, 29.3, 29.1, 29.0, 28.9, 28.4, 27.3 ppm.

4.4.4. Synthesis of CBZ-S-Au

The synthesis of 11-(9H-carbazol-9-yl) undecane-1-thiol (CBZ-SH)-capped Au nanoparticles was performed by first making the Au nanoparticles following the method reported by Peng and co-workers [30]. This was followed by a ligand-exchange process using CBZ-SH (Scheme 2). Using their method for ligand exchange, the substitution was made in the Au nanoparticle solution with a molar ratio of gold/thiol at 1:1.5. The thiol was added to the Au nanoparticles solution in toluene (2 mL) and the solution was further stirred for 30 min and then refluxed for another 30 min. After cooling the solution, the toluene was evaporated to reduce the volume by one third. Next, thiol-coated nanoparticles were precipitated using a minimum amount of methanol. After separating the precipitate from the supernatant, it was redissolved in toluene. The particle dispersion was subjected to precipitation/redispersion to finally afford a black solid product. ¹H NMR was then used to measure the ratio of nonexchanged decanoic acid to exchanged CBZ-SH ligands. This ratio was converted into a fraction of exchanged ligands based on the average decanoic acid Au cluster composition. The exchange was found to be 72 % based on a 5 % NMR confidence limit.

Received: August 26, 2007

Revised: October 15, 2007

- [1] R. Gangopadhyay, A. De, *Chem. Mater.* **2000**, *12*, 608.
- [2] V. L. Colvin, M. C. Schiamp, A. P. Alivisatos, *Nature* **1994**, *370*, 354.
- [3] B. O. Dabbousi, M. G. Bawendi, O. Onitsuka, M. F. Rubner, *Appl. Phys. Lett.* **1995**, *66*, 1316.
- [4] V. Ruiz, P. G. Nicholson, S. Jollands, P. A. Thomas, J. V. Macpherson, P. R. Unwin, *J. Phys. Chem. B* **2005**, *109*, 19 335.
- [5] a) G. D. Hale, J. B. Jackson, O. E. Shmakova, T. R. Lee, N. Halas, *J. Appl. Phys. Lett.* **2001**, *78*, 1502. b) Y. T. Lim, T. W. Lee, H. C. Lee, O. O. Park, *Synth. Met.* **2002**, *128*, 133.
- [6] W. P. Haperin, *Rev. Mod. Phys.* **1986**, *58*, 533.
- [7] C. Suryanarayana, *Int. Mater. Rev.* **1995**, *40*, 41.
- [8] M.-C. Daniel, D. Astruc, *Chem. Rev.* **2004**, *104*, 293.
- [9] a) T. Teranishi, I. Kiyokawa, M. Miyake, *Adv. Mater.* **1998**, *10*, 596. b) I. Pastoriza-Santos, L. M. Liz-Marzán, *Nano Lett.* **2002**, *2*, 903. c) Y. S. Shon, E. Cutler, *Langmuir* **2004**, *20*, 6626.
- [10] C. Burda, X. Chen, R. Narayanan, M. A. El-Sayed, *Chem. Rev.* **2005**, *105*, 1025.
- [11] K. Kneipp, H. Kneipp, I. Itzkan, R. R. Dasari, M. S. Feld, *Chem. Rev.* **1999**, *99*, 2957.
- [12] A. Baba, K. Onishi, W. Knoll, R. Advincula, *J. Phys. Chem. B* **2004**, *108*, 18 949.
- [13] a) W. Chen, W. Cai, L. Zhang, G. Wang, L. Zhang, *J. Colloid. Interf. Sci.* **2001**, *238*, 291. b) M. J. Yang, T. Tsutsui, *Jpn. J. Appl. Phys.* **2000**, *39*, L828. c) C. L. Lee, K. B. Lee, J. Kim, *J. Appl. Phys. Lett.* **2000**, *77*, 2280.
- [14] a) V. N. Bliznyuk, S. A. Carter, J. C. Scott, G. Klarner, R. D. Miller, D. C. Miller, *Macromolecules* **1999**, *32*, 361. b) A. P. Kulkarni, Y. Zhu, S. A. Jenekhe, *Macromolecules* **2005**, *38*, 1553.
- [15] a) C. Xia, R. Advincula, *Chem. Mater.* **2001**, *13*, 1682. b) S. Inaoka, R. Advincula, *Macromolecules* **2002**, *35*, 2426. c) C. Xia, R. Advincula, *Macromolecules* **2001**, *34*, 5854.
- [16] M. Grell, D. D. C. Bradley, G. Ungar, J. Hill, K. S. Whitehead, *Macromolecules* **1999**, *32*, 5810.
- [17] a) S. Deng, R. Advincula, *Chem. Mater.* **2002**, *14*, 4073. b) P. Taranekar, X. Fan, R. Advincula, *Langmuir* **2002**, *18*, 7943. c) M.-K. Park, C. Xia, R. C. Advincula, P. Schutz, F. Caruso, *Langmuir* **2001**, *17*, 7670. d) P. Taranekar, A. Baba, T. M. Fulghum, R. Advincula, *Macromolecules* **2005**, *38*, 3679.
- [18] H. J. Park, T. Y. Lim, O. O. Park, K. J. Yu, W. J. Kim, Y. C. Kim, *Chem. Mater.* **2004**, *16*, 688.
- [19] M. M. Alvarez, J. T. Khoury, T. G. Schaaff, M. N. Shafiqullin, I. Vezmar, R. L. Whetten, *J. Phys. Chem. B* **1997**, *101*, 3706.
- [20] a) A. Henglein, D. Meisel, *Langmuir* **1998**, *14*, 7392. b) A. Henglein, *Langmuir* **1999**, *15*, 6738.
- [21] T. Gu, J. K. Whitesell, M. A. Fox, *Chem. Mater.* **2003**, *15*, 1358.
- [22] R. R. Bhattacharjee, A. K. Das, D. Si, S. Haldar, A. Banerjee, T. K. Mandal, *J. Nanosci. Nanotechnol.* **2005**, *5*, 1141.
- [23] a) F. Mafune, J.-Y. Kohno, Y. Takeda, T. Kondow, *J. Phys. Chem. B* **2001**, *105*, 9050. b) S. I. Hintschich, C. Rothe, S. Sinha, A. P. Monkman, P. Scanducci de Freitas, U. Scherf, *J. Chem. Phys.* **2003**, *119*, 12 017.
- [24] A. P. Kulkarni, X. Kong, S. A. Jenekhe, *J. Phys. Chem. B* **2004**, *108*, 8689.
- [25] a) S. Setayesh, A. C. Grimsdale, T. Weil, V. Enkelmann, K. Mullen, F. Meghdadi, E. J. W. List, G. Leising, *J. Am. Chem. Soc.* **2001**, *123*, 946. b) M. Gaal, E. J. W. List, U. Scherf, *Macromolecules* **2003**, *36*, 4236.
- [26] C. Fan, S. Wang, J. W. Hong, G. C. Bazan, K. W. Plaxco, A. J. Heeger, *PNAS* **2003**, *100*, 6297.
- [27] A. Aguila, R. Murray, *Langmuir* **2000**, *16*, 5949.
- [28] a) R. Chance, A. Prock, R. Silbey, R. Advances in Chemical Physics (Eds: S. A. Rice, I. Prigogine), Vol. 37, **1978**, John Wiley and Sons, New York pp. 1–65. b) D. Waldeck, P. Alivisatos, C. Harris, *Surf. Sci.* **1985**, *158*, 103.
- [29] Y.-Y. Luk, M. L. Tingey, K. A. Dickson, R. T. Raines, N. L. Abott, *J. Am. Chem. Soc.* **2004**, *126*, 9024.
- [30] R. N. Jana, X. Peng, *J. Am. Chem. Soc.* **2003**, *125*, 14 280.